



Insitu Measurement of Damping of Soils

W.P. Stewart and R.G. Campanella
Graduate Student and Professor, Department of Civil
Engineering, University of British Columbia, Vancouver, B.C.,
Canada

SYNOPSIS: The Seismic Cone Penetration Test (SCPT) has been shown to give reasonable results for insitu measurements of shear wave velocity, and this paper extends this work to include measurements of damping. The relevant equations of motion are described, factors affecting amplitude decay are discussed, and the nature of damping is summarized. Consideration is given to some of the practical aspects of pre-processing of signals. Three methods of damping calculation are presented. The first two, attenuation coefficient and modified SHAKE methods, require the application of amplitude corrections, which is not straight-forward, give variable results, and indicate negative damping in a clayey silt layer. The third, the spectral slope method eliminates the need for amplitude corrections and gives less variable and more acceptable results. The spectral slope method gave damping measurements of about 2% to 3% for sand and 0.3% to 0.5% for silt, at low strain levels of 10^{-4} to 10^{-3} %.

INTRODUCTION

Ground response analysis requires a mathematical model of sub-surface soils at a site. Numerous models have been developed but all basically require some variation of the values of the shear modulus and damping (attenuation) of the soil. Traditionally damping has been measured in the laboratory. However it is difficult to ensure that the tests are representative of field conditions. As Mok et al. (1988) stated: "These can be highly questionable assumptions." Therefore it is desirable to develop insitu methods that can provide more direct measurements of damping to complement the results of laboratory tests.

Seismic cone penetration testing (SCPT) techniques have been under development at UBC since 1980 (Campanella and Robertson, 1984). Typically shear waves are generated by striking a weighted beam horizontally, and recording the resultant signals at depth increments of 1m. The initial emphasis was on low-strain shear wave velocity measurements, which allow the calculation of the maximum shear modulus based on elastic wave theory. This paper extends the technique to damping measurements. A number of authors have presented papers on insitu damping measurements including: Woods(1978), Shannon and Wilson(1980), Tonouchi et al. (1983), Hoar and Stokoe (1984), Redpath and Lee(1986), and Mok et al.(1988). These tests took place in pre-bored, lined holes using crosshole or downhole methods.

A brief review of body waves is first presented here, followed by a discussion of damping. Three methods of damping calculation are then presented. Downhole seismic cone test results and analyses are presented and compared.

DOWNHOLE SHEAR TESTS

A portion of a typical suite of processed records is shown in Fig.1. A repeatable shear beam source was used to generate signals, which were recorded on a moveable accelerometer mounted in a cone. Fig.1 shows the first cycle of the shear wave recorded at seven different depths. At this site the upper portion (to about 15m depth) is primarily sand, and the lower portion (below about 17m) is primarily clayey silt. The signal peaks show a rapid attenuation in the shallow sands, and less rapid attenuation in the deeper silts.

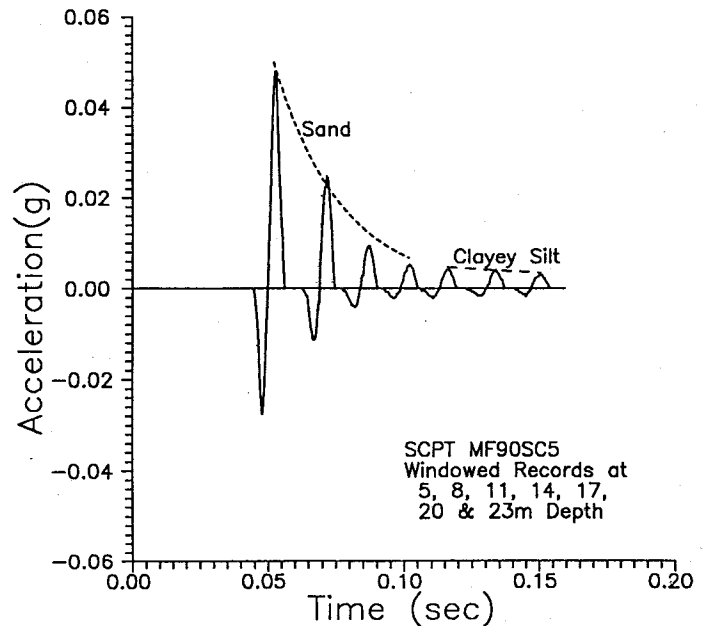


Fig.1. Portion (7 depths) of suite of processed accelerometer records.

The peak strain levels, s_p , caused by the shear waves can be calculated from the peak particle velocity, V_m , (calculated by integrating the accelerometer record) and the measured shear wave velocities, V_s , using the equation given by White(1965):

$$s_p = V_m / V_s \quad (1)$$

The relatively low strain levels decrease with depth, from about $1.4 \times 10^{-3}\%$ at 5m to $1.0 \times 10^{-4}\%$ at 25m.

BODY WAVES

This section will introduce the equations describing body waves and discuss factors affecting the amplitudes of such waves. First consider a simple sine wave with no damping travelling along a string with wavelength L and velocity v , then:

$$A = A_0 \sin \frac{2P_i}{L} (x-vt) ; P_i = 3.14159... \quad (2)$$

It is convenient to introduce the following terms:

$$\text{wave number, } k = \frac{2P_i}{L} \quad \text{and angular frequency,}$$

$$w = \frac{2P_i}{T}$$

where T is the period; and, to allow for phase shifts:

$$\text{phase, } \theta = \text{initial value of phase angle.}$$

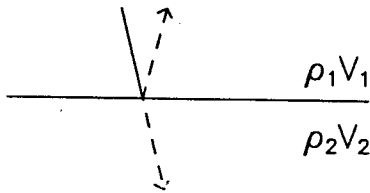
Then the above equation becomes:

$$A = A_0 \sin(kx-wt-\theta) \quad (3)$$

or, in terms of the complex exponential:

$$A = A_0 \exp[i(kx-wt)] \quad (4)$$

TRANSMISSION (REFLECTION)



DIVERGENCE

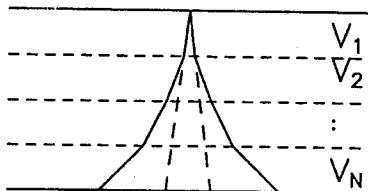


Fig.2. Causes of amplitude changes at interfaces between soil layers.

This equation is for one-dimensional motion, in direction x only, such as along a string. Waves in soil can be plane waves, for example generated by an earthquake movement of flat-lying bedrock, or spherical waves, for example generated by a point source explosive device, or in general, a mix of these two wave types. For spherical waves in a homogeneous medium, neglecting near-field terms, White(1965) showed that the amplitude decayed inversely with distance, R i.e.

$$A = A_0 1/R \exp[i(kx-wt)] \quad (5)$$

However, soil is rarely homogeneous and commonly layered. At the interface between two layers, the amplitude of spherical body waves can be affected in at least two ways: transmission/reflection and divergence. As shown in Fig.2 the amplitude of the transmitted wave is reduced because (1) part of the wave energy is reflected (for both plane and spherical waves), and (2) the wave front of spherical waves is refracted, decreasing the amplitude for increasing velocities.

The attenuation correction for transmission is a function of the change in acoustical impedance across an interface. The acoustical impedance of a layer is the product of the density, ρ and velocity, V . The reflection coefficient, r , of the boundary between layers 1 and 2, is given by:

$$r_{12} = (\rho_2 V_2 - \rho_1 V_1) / (\rho_2 V_2 + \rho_1 V_1) \quad (6)$$

and since the variation in density is often smaller than the variation in velocity, the reflection coefficient is often given as approximately $(V_2 - V_1) / (V_2 + V_1)$. The transmission coefficient, t , is given by $t_{12} = 1 - \text{Abs}(r_{12})$, and t_{12} is the attenuation correction.

The attenuation correction for divergence is somewhat more complex, and has been discussed by Mack(1966). Although it is not stated, the development is based on the principle of refraction as given by Snell's Law;

$$\frac{\sin(a_1)}{\sin(a_2)} = \frac{V_1}{V_2} ; \text{ where } a = \text{angle of incidence} \quad (7)$$

The energy density ratio, e , will be given by the ratio of the areas with and without refraction. Since the energy is proportional to the square of the wave amplitude, the amplitude correction will be equal to the square root of e . If the region of interest consists of N horizontal layers of constant velocity V_n , over the depth from Z_1 to Z_2 , then the attenuation correction at a depth of Z_2 is given by the reciprocal of:

$$\frac{1}{(Z_2 - Z_1) V_1} \sum_{n=1}^N (V_n Z_n)$$

For his problem, Mack found the divergence factor to be $1/1.15$, compared with $1/1.21$ for the effects of reflection.

Although the SCPT provides a detailed soil profile (Robertson et al., 1986), it is not practical to assign numerical values of both density and shear wave velocity to the numerous thin layers outlined in a typical profile. For

purposes of the calculations outlined below, it was decided to assume that the soil density could be considered constant, and that the effective soil layering could be based on the velocities measured at each metre of depth. On this basis it is straight forward to calculate the reflection, divergence, and spherical spreading corrections with depth. A typical example of a velocity profile (at the site of the records given in Fig.1) is shown on Fig.3. The corresponding amplitude reduction factors due to transmission, divergence and the combined effects are shown in Fig.4. The combined effect is used for further calculations. This approach assumes spherical wave-fronts. Although this is not strictly true, especially near the surface, the approximation becomes better with depth. It should be noted that the points for the combined effect, in the upper portion, can be approximated by a power law varying with depth as $R^{1.65}$.

NATURE OF DAMPING

Material damping refers to the energy dissipation within a soil mass during dynamic (cyclic) loading. Whitman (1970) provided one of the earlier summaries of material damping of soils (internal damping, intrinsic damping, or simply damping). The stress-strain curve during unloading is not the same as that during loading, giving rise to a closed hysteresis loop. The area of the loop is a measure of the energy lost during a cycle of unloading/reloading. Whitman expresses the damping capacity, d_{cap} as:

$$d_{cap} = \frac{\text{ratio of energy lost in cycle to maximum strain energy introduced in cycle}}{= A_{loop}/A_{tri}} \quad (8)$$

where: A_{loop} = Area of loop of stress-strain curve
 A_{tri} = Area of right triangle between strain axis and line from origin to point of loop.

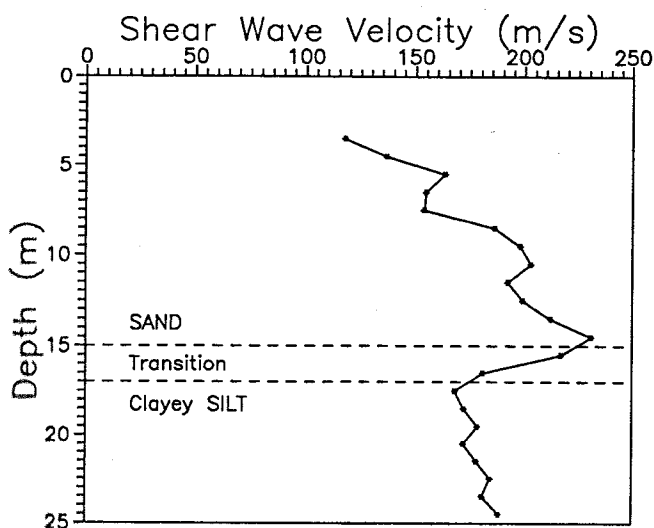


Fig.3. Shear wave velocity profile.

For purposes of analysis, he related d_{cap} to viscous damping parameters (for small damping levels):

$$\text{logarithmic decrement, } d_{log} = d_{cap}/2 \quad (9)$$

$$\text{loss coefficient (phase lag between force and displacement), } d_{loss} = d_{cap}/(2P_i) \quad (10)$$

$$\text{(in general } d_{cap} = 2P_i \tan(d_{loss})$$

$$\text{damping ratio (ratio of actual viscous coefficient to critical value), } D = d_{cap}/(4P_i). \quad (11)$$

This last definition is commonly used in geotechnical engineering models and is often referred to as the percentage of critical damping. This definition will be used in this paper.

In the geophysical literature, damping is often referred to as the quality factor, Q , or as the dissipation factor, $1/Q$, and Q is defined as the ratio of stored energy to dissipated energy. It can be shown that critical damping is related to Q by:

$$D = [1 + (2Q)^2]^{-1/2}, \text{ or approximately } D = 1/2Q \quad (12)$$

Whitman noted that the most important factors affecting damping, at least in sands, are shear strain and confining pressure. There was a slight increase in damping when water was introduced to dry sand, and damping in clay appeared to be less than in sand. Typical laboratory values of damping at small strains are given in Table I.

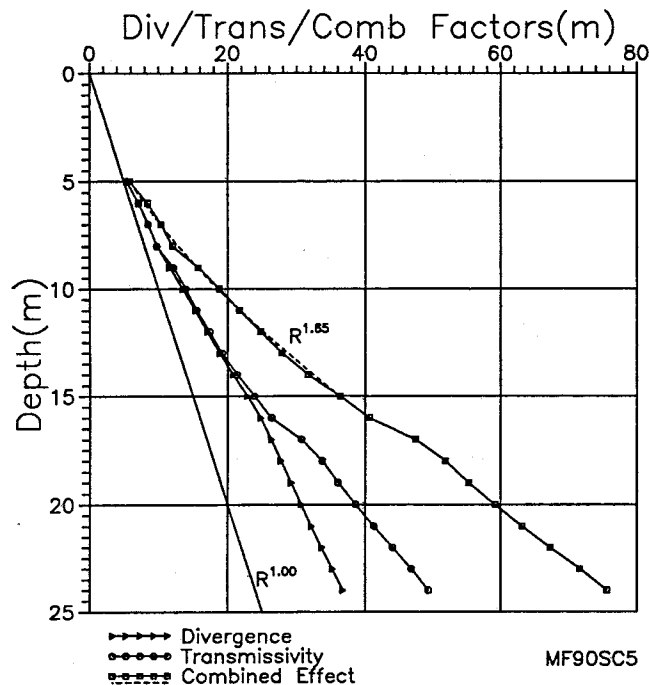


Fig.4. Amplitude correction factors based on velocity profile.

TABLE I. Laboratory Measurements of Damping

Soil Type	Strain,%	Damping,%	Source
Cohesionless	10 ⁻⁴ -10 ⁻³	0.5-2	Seed et al.,1986
Cohesive	10 ⁻³	3 (1-5)	Sun et al.,1988
Sand	10 ⁻³	1	Saxena and Reddy,1989
Sand	10 ⁻³	1.5	Ishihara,1982
Clay	10 ⁻³	1.5-2	Zavoral,1990
Sand	10 ⁻³	0.5-1	Zavoral,1990

In order to do calculations using field measurements, it is necessary to consider the equation of motion. Johnston and Toksoz(1981) show that damping can be introduced into equation (1) by making w or k complex, i.e.

$$k = k_r + i\theta, \text{ where } \theta = \text{attenuation coefficient.} \quad (13)$$

Then the expression for the real component of amplitude becomes:

$$A = A_0 1/R \exp(-\theta R) \quad (14)$$

Mok et al.(1988) used this expression, considering two signals of amplitude A₁,A₂ at distances of R₁,R₂ from the source, to yield:

$$\theta = \ln(A_1 R_1 / A_2 R_2) / (R_2 - R_1) \text{ or} \quad (15)$$

$$D = \ln(A_1 R_1 / A_2 R_2) / (2P_i t_f) \quad (16)$$

where: t_f = interval travel time
f = frequency of wave.

Tonouchi et al.(1983) used a downhole method with a shallow fixed receiver and moving deeper receiver, and computed the attenuation coefficient from:

$$\theta = \frac{\ln\left\{ \frac{(R_1 B_{1f} / A_{1f})}{(R_2 B_{2f} / A_{2f})} \right\}}{R_2 - R_1} \quad (17)$$

where: A_{1f}, A_{2f} = FFTs of shallow signals for hits 1&2
B_{1f}, B_{2f} = FFTs of deeper signals
FFT = Fast Fourier Transform of signal

A similar type of equation is used in the computer program SHAKE (Schnabel et al., 1972):

$$u = E \exp[i(kx + wt)] + F \exp[-i(kx - wt)]. \quad (18)$$

The amplitude coefficients (E,F) are calculated using the soil density and complex shear modulus G* given by:

$$G^* = G(1 + 2iD) \text{ (original version)} \quad (19)$$

$$G^* = G(1 - 2D^2 + 2iD[1 - D^2]^{1/2}) \text{ (revised version -Udaka and Lysmer, 1973)} \quad (20)$$

Redpath and his colleagues (1982,1986) used a similar approach except that they define the attenuation coefficient θ as zf or z = θ/f.

Therefore equation (14) becomes:

$$A = A_0 1/R \exp(-zfR) \quad (21)$$

If we consider signals measured at two distances from the source, R₁ and R₂ where R₂ is greater than R₁, then the ratio is:

$$\frac{A_2}{A_1} = \frac{R_1}{R_2} \exp[-zf(R_2 - R_1)] \quad (22)$$

Taking natural logarithms of this equation gives:

$$\ln \frac{A_2}{A_1} = \ln \frac{R_1}{R_2} - zf(R_2 - R_1) \quad (23)$$

Differentiating these terms with respect to f gives:

$$d[\ln(A_2/A_1)] / df = -z(R_2 - R_1) \quad (24)$$

It can be noted that the term given as 1/R in equation (21) is eliminated by differentiating. Any geometric term affecting the amplitude that does not depend on frequency will be similarly eliminated. This will include the transmission and reflection corrections described above if the velocities are independent of frequency, which is the case if the frequency range for the analysis is properly selected. If R₁ is held constant and R₂ (or simply R) is varied, we can differentiate with respect to R, giving:

$$\frac{d^2[\ln(A_2/A_1)]}{df dR} = -z \quad (25)$$

Some reported field measurements of damping are given in Table II.

TABLE II. Field Measurements of Damping

Soil Type	Damping,%	Source
Sand	6	Kudo and Shima,1981
Silt	2.5	"
Alluvium	12(<25m)	Redpath et al.,1982
(Sand & Clay)	3.5(deeper)	(lab.1.5-3.5%)
Sandy	5	Tonouchi et al.,1983
Clayey	1.7	"
Fine sand	1.7	"
Sandy silt	2.5	"
Sand	4	Meissner and Theilen,1986
Bay mud	4	Redpath and Lee, 1986
		(lab. 2.5%)
Clay	4-7	Mok et al.,1988
Sand(P-wave)	2-3	" (lab. 0.7%)

SIGNAL PROCESSING CONSIDERATIONS

Before describing the calculation methods used, it is necessary to give some consideration to general procedures in handling the data. A fairly typical signal is shown in Fig.5a. It can be seen that, in addition to the main pulse, there is noise before and after, and that there are additional smaller pulses after the main pulse. The nature of the smaller pulses is a matter of present research, however it is

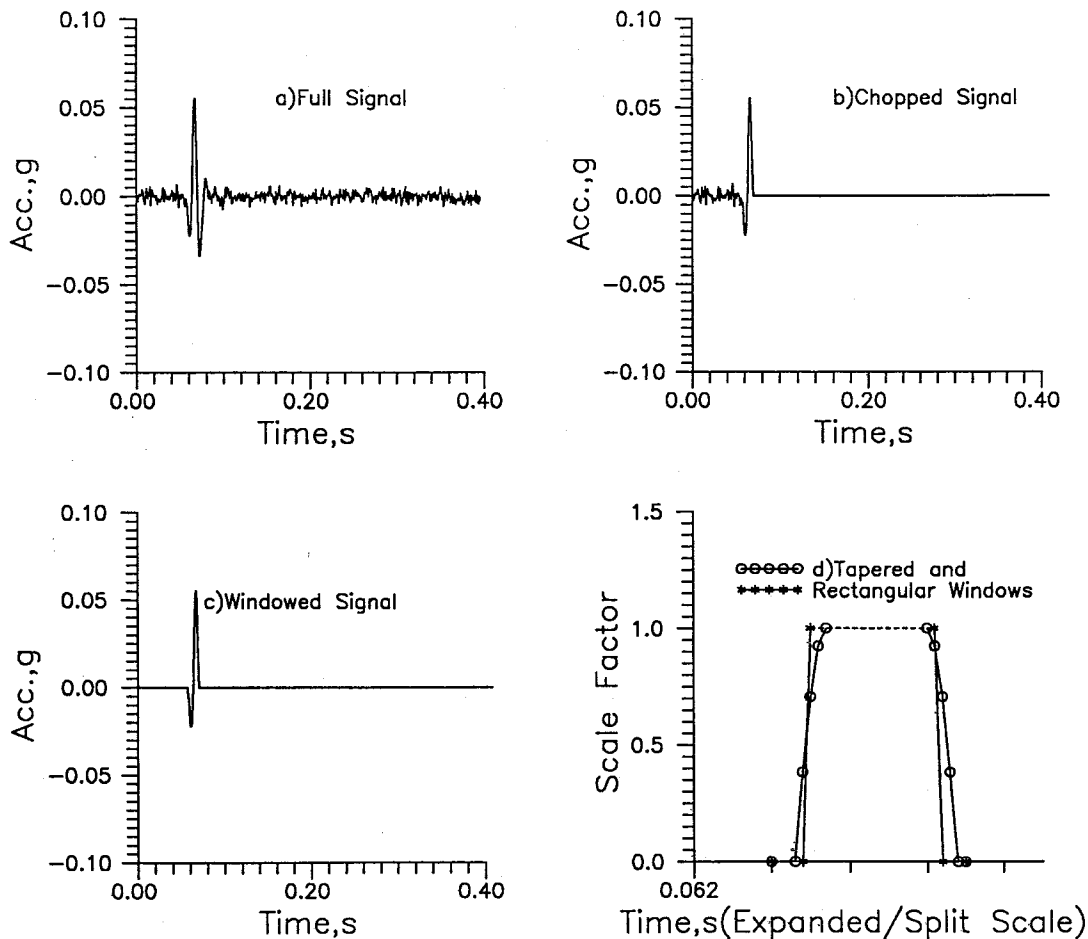


Fig.5. Signal windowing.

apparent that they affect the spectrum (see Fig.6) and consideration must be given to these effects, by pre-processing of the signals.

The concept of windowing is of great importance in the spectral analysis of signals (Bath, 1974; Oppenheim et al., 1983). A window signal is formed along the same time scale as the original signal and a scale factor ranging from 0 to 1 is assigned at each time step. Windowing is simply the operation of multiplying the original signal by the window signal. The simplest window is the Uniform window, which has the value 1 at all time steps, and has no effect on the signal. A wide variety of window types; Bartlett, Hanning, Hamming, Flattop, Exponential, etc. have been developed for periodic signals. However these window types will distort transient signals, such as those measured for this work, and must not be applied. It is simply desired to remove those parts of the signal that are extraneous to the measurement.

The next simplest window is a step function which has a value of 1 up to the end of the main pulse and 0 for the balance of the time period. Multiplying the original signal by this step window gives the chopped signal in Fig.5b. A rectangular window (see Fig.5d) has a value of 1 for the duration of the main pulse only and 0 before and after. Applying the rectangular

window gives the windowed signal in Fig.5c. The FFT of a rectangular window contains ripples (Gibb's phenomenon), so that a tapered window (see Fig.5d) is sometimes used. Mok et al.(1988) used an "extended cosine-bell" (tapered) window for their geophone records. However if the ends of a rectangular window are applied at the zero-crossings at each end of the main pulse, the ripple effects are essentially multiplied by zero, and the effect is negligible. For our accelerometer records, a simple rectangular window with the ends at the zero crossings seemed to provide satisfactory results. The frequency domain results (FFTs) of such processing are shown in Fig.6. The full signal is quite irregular in the range of interest (about 40 to 100Hz), whereas the chopped and windowed signals are smoother and quite close to one another.

It is also necessary to determine the bandwidth in the frequency domain to be used for further calculations. One method of determining a suitable band width is to use the coherence function. Use of this method requires repeated hits at the same depth. Typically four hits at each depth have been used. The coherence function is defined as:

$$\text{Coh} = \frac{G_{yx} G_{yx}^*}{G_{xx} G_{yy}} \quad (26)$$

where: G_{yx} = Average of Cross-Correlation Spectra
 G_{yx}^* = Complex Conjugate of G_{yx}
 G_{xx} = Average of Autocorrelations of Upper Signal
 G_{yy} = Average of Autocorrelations of Lower Signal

Using the averages of several signals, it can be shown (Hewlett Packard, 1985) that the coherence can be expressed as:

$$\text{Coh} = \frac{|H|^2 G_{xx}}{|H|^2 G_{xx} + S_n^2} \quad (27)$$

where: $|H|$ = Magnitude of transfer function
 S_n = Average of noise spectra

Thus the coherence will be high at those frequencies where the effect of noise is minor, and it will be low where the noise dominates the signals.

Typical plots of the coherence function are shown in Fig.7. For the signals at shallow depth (5 to 6m), the coherence is very high (essentially 1.0) from about 30 Hz to 150 Hz. For the signals at greatest depth, the coherence is reasonably high (0.98 or greater) from about 40Hz to 105Hz. To allow a consistent approach throughout the depth of the profile, a band width of 40 to 100 Hz was used for all calculations. The choice of an acceptable coherence level will depend on the quality of the signals recorded. Generally a value of 0.95 or greater has been achieved over a reasonably wide bandwidth.

DAMPING CALCULATIONS

Three separate methods of damping calculation are presented based on the above concepts. The first is the attenuation coefficient method, a variation of the approach given by Mok et al.

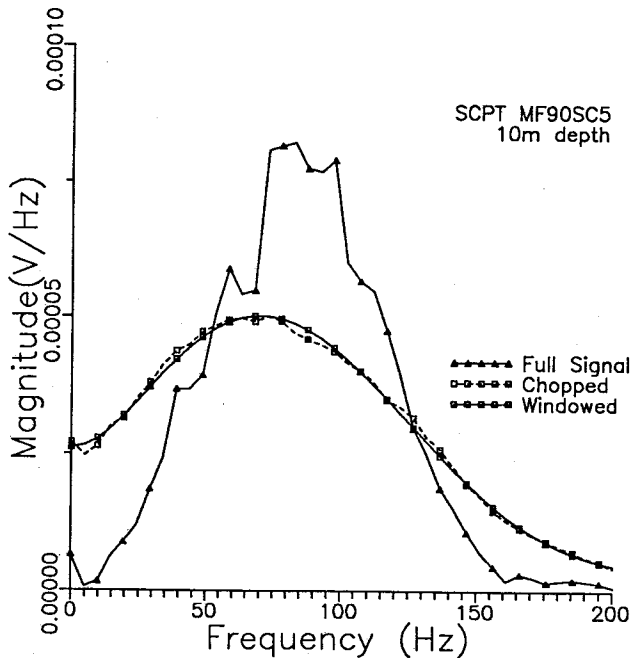


Fig.6. Effect of windowing on FFT of signal.

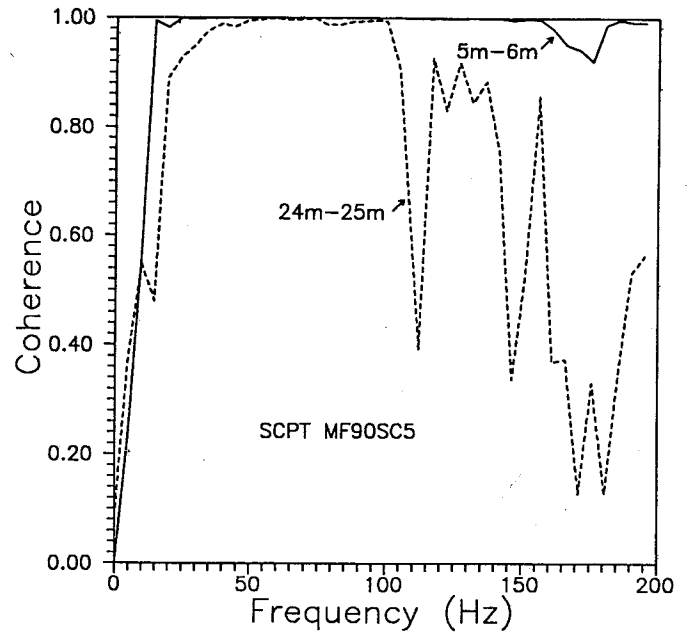


Fig.7. Coherence function at two depth intervals.

(1988), the second is based on a modified version of the SHAKE program, and the third is the spectral slope method as used by Redpath and colleagues (1982, 1986) and others (Kudo and Shima, 1981, Meissner and Theilen, 1986).

Attenuation Coefficient Method

This method makes use of equation (16) which Mok et al. (1988) used directly. However, they were using a crosshole technique and the generated waves were unlikely to encounter interfaces between layers of soil (although the method would be affected by nearby layers of high velocity). In the downhole technique, the generated waves can be expected to pass through soil layers and the transmission and divergence effects described above must be considered. However, in order to use all of the available data, it is necessary to calculate the damping on a metre by metre basis, and the corrections can only be calculated on the same basis. It will be assumed that only one interface (amplitude change) occurs within each interval, for one set of calculations, and that no interfaces occur (no correction) for a second set of calculations. The results of one calculation are shown in Fig.8, and show a slight decline in damping with frequency (about 0.01%/Hz) over the selected frequency range of 40 to 100Hz and a value of 3.4% at the middle of this range. Calculations at other depths showed that the damping variation with frequency could be positive or negative. Results for a series of depths are shown in Fig.9, and indicate a large scatter (-7.6% to 7.0%), with a mean of 3.3% in the upper sands and -1.1% in the lower silts. The results also suggest a fairly constant average value with depth in the upper portion and an increase with depth in the lower portion. Also shown in Fig.9 is the effect of ignoring the transmission/divergence corrections which increases the damping by 0.4% to 8.0%, averaging about 2.9% in the upper portion and

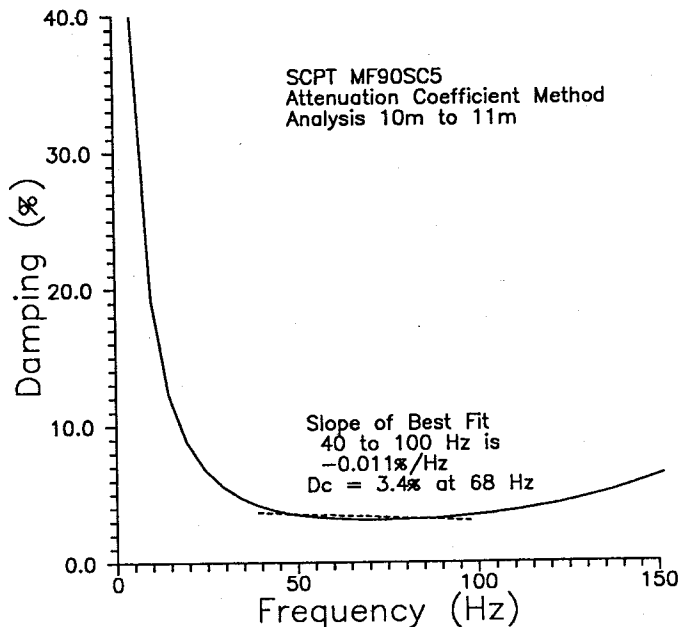


Fig.8. Damping by attenuation coefficient method for 10-11m depth interval.

0.8% in the lower portion. It would appear that, to obtain somewhat reasonable results, it is necessary to include the transmission/divergence corrections in the upper sand, but to neglect the corrections in the lower silts.

The difficulty of applying the interface corrections and the wide scatter in the results, including negative values, makes the attenuation coefficient method difficult to use.

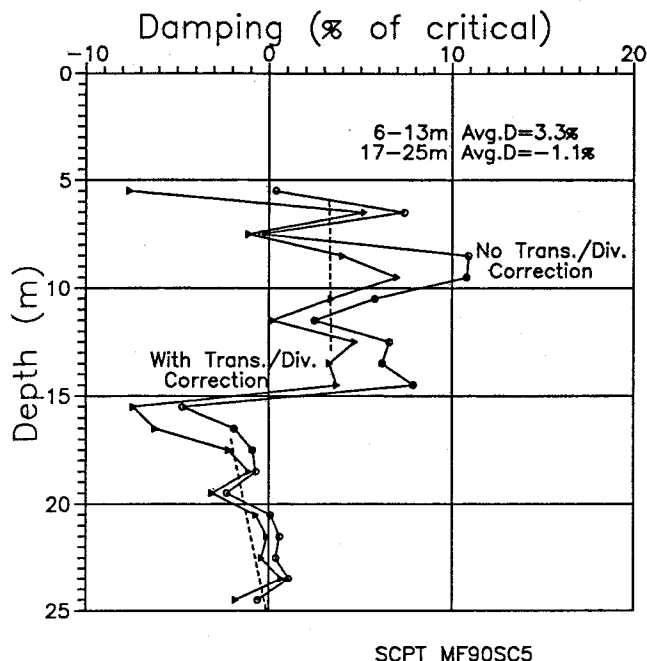


Fig.9. Damping by attenuation coefficient method over seismic cone profile.

Modified SHAKE Method

This second method is based on a modified version of the SHAKE program. The original program was designed primarily to model earthquake motions moving upward from bedrock (Schnabel et al., 1972). The program does allow input of motions at an intermediate level in the soil, but the wave then spreads both up and down. In order to model the downhole tests, it is necessary to force the wave to spread only downwards. This can be done by setting the coefficient E in equation 4 equal to zero. In order to model the spherical wave in a layered soil, it is also necessary to make the transmission and divergence corrections as in the first method. The value of damping is first estimated, and the acceleration response from the program is compared to the observed acceleration record at the greater depth. The damping is then adjusted to give a "best-fit" between the calculated and observed records.

Fig.10 shows the result of a calculation between depths of 10 and 11 metres. For this depth a damping of 5.5% was required to match the calculated peak to the measured peak. The results of a series of calculations for one seismic cone profile is shown in Fig.11. There is again a wide scatter in the results, averaging 4.1% in the upper sands, and -2.8% in the lower silts. The results suggest an increase in damping with depth in both the sands and silts. Calculations were also made for this method ignoring the transmission/divergence corrections and these gave changes very similar to the first method. Also shown on Fig.11 are the results from a series of calculations with essentially no filtering of the signal (1000 Hz low pass filter). The trend of the results is very similar, but the oscillations are reduced.

This method was found to be very time-consuming, compared to the other two methods. The signals

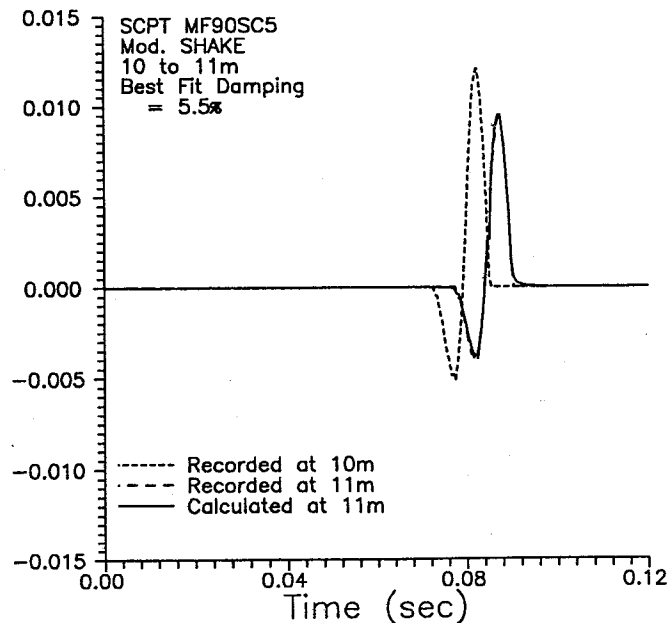


Fig.10. Damping by modified SHAKE method for 10-11m depth interval.

first had to be converted to the format required for the SHAKE program, then iteration of the damping values was performed. The other two methods were written into "macros" with the program VU-POINT which can read the signals directly as collected.

As for the first method, the difficulty of applying the interface corrections and the wide scatter in the results, including negative values, makes the modified SHAKE method difficult to use.

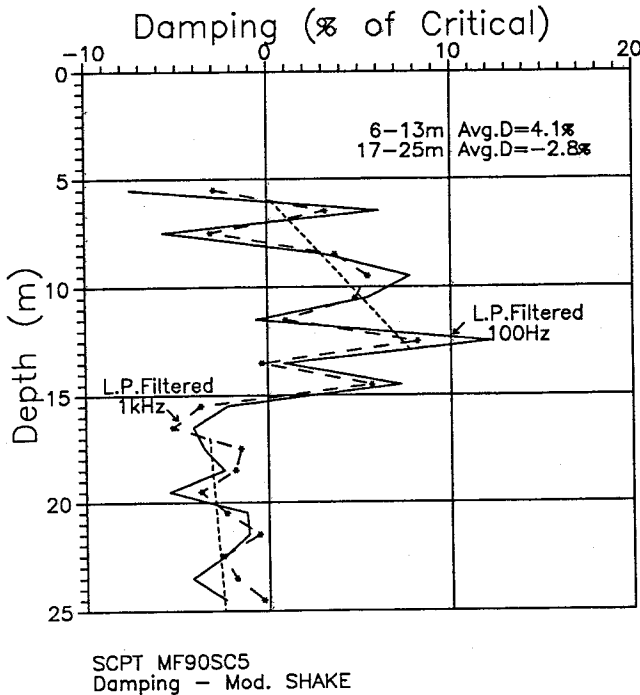


Fig.11. Damping by modified SHAKE method over seismic cone profile.

Spectral Slope Method

The third method used was the spectral slope method, based on equation (25). The coefficient z can be determined by first finding the FFT of one signal at a reference depth, then for each deeper signal compute the FFT, the ratio of the FFTs, and the negative of the natural logarithm (\ln) of the ratio. After finding the slope of $-\ln(\text{ratio})$ versus frequency plot at each depth (see Fig.12), these slopes are plotted versus depth (see Fig.13). An indication of the variability in application of the method can be obtained from the standard deviation of the fit to the slopes of the curves. For the $-\ln(\text{ratio})$ versus frequency plots, the standard deviation was typically 4% to 5% of the slope value. For the upper sands, the fit of the slope of the depth plot had a standard deviation of 7.7%, whereas for the lower clayey silts the standard deviation was about 35%. Except for this last value, the standard deviations are a small fraction of the computed values. The large last value is likely caused by the small damping in the clayey silt.

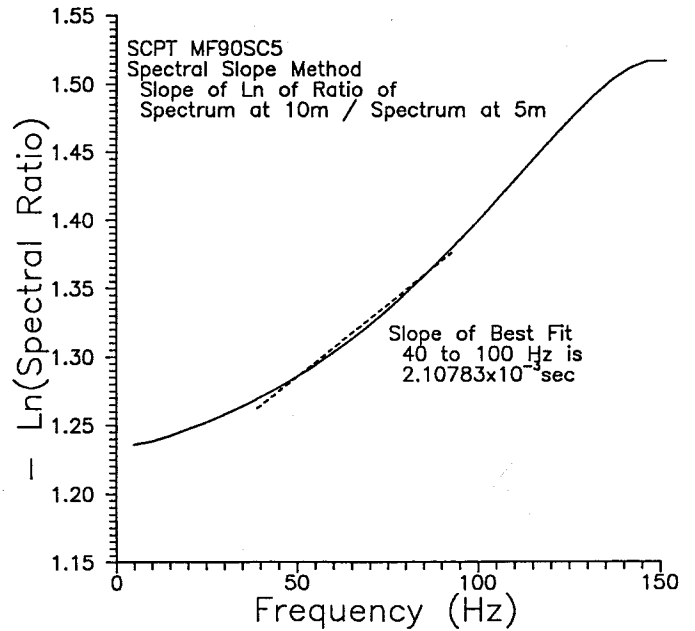


Fig.12. Damping by spectral slope method for 10-11m depth interval.

The slope(s) of the depth plots give the coefficient z for each layer. The fraction of critical damping can be computed as:

$$D = \frac{zV}{2P_1} \quad (28)$$

As shown in Fig.13, the method gives a damping value of 2.2% for the upper sands, and 0.5% for the lower silts. Another SCP Test in the general area gave 3.3% damping for the sands and 0.3% damping for the silts.

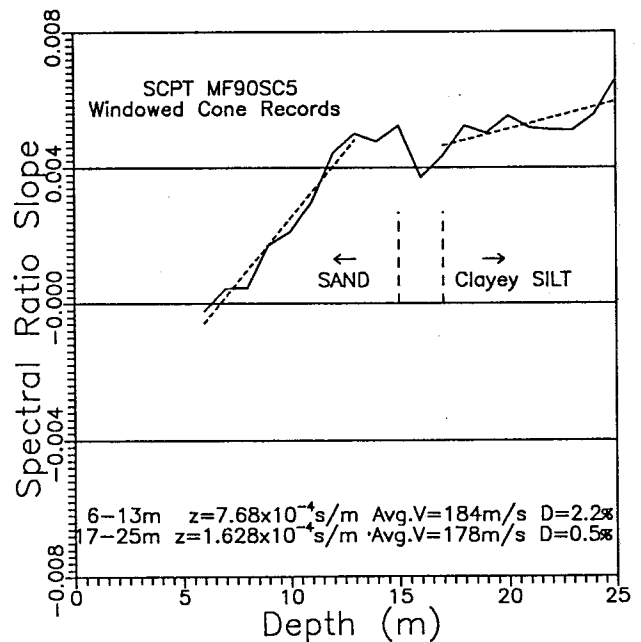


Fig.13. Damping by spectral slope method over seismic cone profile.

The spectral slope method avoids the need for interface corrections and gave relatively low scatter in the results. The damping values reported here are slightly less than other field results reported (about 2% to 6% for sand and about 2% to 4% for cohesive soils). The damping values reported here are higher than laboratory results for the sand (0.5% to 2%), but lower than those for cohesive soils (1% to 5%).

SUMMARY

The equations of motion relevant to damping calculations have been described, factors affecting amplitude decay were discussed, and the nature of damping has been summarized. Some practical aspects of pre-processing of signals were discussed. Three methods of damping calculation were presented. The first two, attenuation coefficient and modified SHAKE methods, required the application of amplitude corrections, which is not straight-forward, gave variable results, and indicated negative damping in the lower clayey silt layer. The third, the spectral slope method eliminated the need for amplitude corrections and gave less variable results. The method gave damping of about 2% to 3% for the upper sand layer and 0.3% to 0.5% in the silt.

Based on these results, the spectral slope method is the most promising approach to insitu measurement of damping. Seismic cone profiles in sand, analyzed with this method, gave results between those reported for field and laboratory tests. Further research is required to establish the validity of these measurements. Further research is being conducted presently to investigate the nature of the secondary pulses in the signals, and the effect on damping calculations.

ACKNOWLEDGEMENTS

The authors wish to acknowledge the financial support of the Natural Sciences and Engineering Research Council Strategic Grant for this study. The first author also wishes to acknowledge the GREAT scholarship provided by the Science Council of B.C. in cooperation with Conetec Investigations Ltd. The efficient support of the technical staff of the Civil Engineering Department of the University of British Columbia is appreciated and was essential in order to carry out the research described.

REFERENCES

- BATH, M. 1974. Spectral analysis in geophysics. Elsevier Scientific Pub. Co., New York.
- CAMPANELLA, R.G. and ROBERTSON, P.K. 1984. A seismic cone penetrometer to measure engineering properties of soil. 54th Annual Meeting, Soc. Exp. Geop., Atlanta, Ga., Dec.
- HEWLETT PACKARD 1985. The fundamentals of signal analysis. Application note 243. Feb.
- HOAR, R.J. and STOKOE, K.H. II 1984. Field and laboratory measurements of material damping of soil in shear. Proc. 8th World Conf. on Earthquake Eng., San Francisco. Vol. III, pp. 47-54.
- ISHIHARA, K. 1982. Evaluation of soil properties for use in earthquake response analysis. Int. Symp. on Numerical Models in Geomechanics. Zurich.
- JOHNSTON, D.H. and TOKSOZ, M.N. 1981. Definitions and terminology. in Seismic Wave Attenuation. Geophysics reprint series No.2. Soc. Exp. Geophy. pp.1-5.
- KUDO, K. and SHIMA, E. 1981. Attenuation of shear waves in soil. in Seismic Wave Attenuation. Geophysics reprint series No.2. Soc. Exp. Geophy. pp.325-338.
- MACK, H. 1966. Attenuation of controlled wave seismograph signals observed in cased boreholes. Geophysics, Vol. XXXI, No.1, Feb., pp. 243-252.
- MOK, Y.J., SANCHEZ-SALINERO, I., STOKOE, K.H. II, and ROESSET, J.M. 1988. In situ damping measurements by crosshole seismic method. Earthquake Eng. and Soil Dynamics II. ASCE Spec. Conf., Park City, Utah. pp.305-320.
- MEISSNER, R. and THEILEN, F. 1986. Experimental studies of the absorption of seismic waves. in "Absorption of Seismic Waves (ASW)". DGMK-Project 254. DGMK, Hamburg.
- OPPENHEIM, A.V., WILLSKY, A.S., and YOUNG, I.T. 1983. Signals and systems. Prentice-Hall Inc., Englewood Cliffs, N.J.
- REDPATH, B.B., EDWARDS, R.B., HALE, R.J., and KINTZER, F.C. 1982. Development of field techniques to measure damping values for near-surface rocks and soils. Prepared for NSF Grant No. PFR-7900192.
- REDPATH, B.B. and LEE, R.C. 1986. In-situ measurements of shear-wave attenuation at a strong-motion recording site. Prepared for USGS Contract No. 14-08-001-21823.
- ROBERTSON, P.K., CAMPANELLA, R.G., GILLESPIE, D., and RICE, A. 1986. Seismic CPT to measure insitu shear wave velocity. J. Geotech. Eng. Div., ASCE, Vol. 112, No. 8, pp. 791-804.
- SAXENA, S.K. and REDDY, K.R. 1989. Dynamic moduli and damping ratios for Monterey No. 0 sand by resonant column method. Soils and Foundations. Vol. 29, No. 2, June, pp. 37-51.
- SCHNABEL, P.B., LYSMER, J., and SEED, H.B. 1972. SHAKE, a computer program for earthquake response analysis of horizontally layered sites. Report No. EERC 72-12. College of Eng., UC Berkeley.
- SEED, H.B., WONG, R.T., IDRIS, I.M., and TOKIMATSU, K. 1986. Moduli and damping factors for dynamic analyses of cohesionless soils. JGED, ASCE, Vol. 112, No. 11, Nov., pp. 1016-1032.
- SHANNON and WILSON INC. 1980. Evaluation of insitu damping characteristics. Prepared for U.S. Nuclear Reg. Comm., NUREG/CR-1638.

- SUN, J.I., GOLESORKHI, R., and SEED, H.B. 1988. Dynamic moduli and damping ratios for cohesive soils. Report No. UCB/EERC-88/15. EERC UC Berkeley.
- TONOUCHI, K., SAKAYAMA, T., and IMAI, T. 1983. S wave velocity and the damping factor. Bull. Int. Assoc. Eng. Geol. No.26-27, Paris. pp.327-333.
- WHITE, J.E. 1965. Seismic waves. McGraw-Hill, New York.
- WHITMAN, R.V. 1970. Site evaluation and dynamic analysis of nuclear power plants. M.I.T. Press.
- WOODS, R.D. 1978. Measurement of dynamic soil properties. ASCE GED Speciality Conf. on Earthquake Eng. and Soil Dynamics. Pasadena, CA. Vol.1, pp.91-178.
- UDAKA, T. and LYSMER, J. 1973. Supplement to computer program SHAKE. EERC UC Berkeley.
- ZAVORAL, D. 1990. Dynamic properties of an undisturbed clay from resonant column testing. Civil Engineering Dept., M.A.Sc. Thesis, University of British Columbia.